

Proceedings of the Korean Nuclear Society Autumn Meeting
Seoul, Korea, October 1999

Consistent 1-D Neutronics Modeling using Current Conservation Factors

Kibog Lee, Han Gyu Joo, Byung-Oh Cho and Sung Quun Zee
Korea Atomic Energy Research Institute
P.O. Box 150, Yusong, Taejon, 305-600, Korea

Abstract

The 3D neutronics code is the ultimate means of achieving high fidelity in the neutronic simulation of the reactor core, nevertheless the 1D neutronics model is needed to replace 3D model in many practical circumstances.

In this paper a 3D consistent 1D model based on nonlinear analytic nodal method is developed. During the derivation, the current conservation factor (CCF) is introduced which guarantees the same axial neutron currents obtained from the 1D equation as the 3D reference values.

To test the 1D model with CCF, three cases of steady state calculation were performed and compared with 3D reference values. The errors of K-eff values were reduced about one tenth when using CCF. And the errors of power distribution were decreased to the range of one fifth or tenth at steady state calculation.

With the planar averaged group constants and the CCF's introduced in this paper, it becomes possible to reproduce the 3D reference solution from the 1D model. Thus the 1D model with CCF can provide the preciser results at the steady state, and it is expected that the slow transient such as the day range xenon dynamics can be simulated more accurately with 1D model.

I. Introduction

The 3D neutronics code is the ultimate means of achieving high fidelity in the neutronic simulation of the reactor core, nevertheless the 1D neutronics model is needed to replace 3D model in many practical circumstances. The needs are two folds; 1) the significant reduction in computing time and 2) the circumventing the lack of detailed neutronic data for 3D model. When the core characteristic parameters are predominant in the axial direction and the radial flux shape has negligible effects on the global behavior such as the cases of uncontrolled bank withdrawal, xenon transient,

BWR flow instability etc, the 1D model can be useful.

In the case that a 3D model is available and a 1D modeling is desired for execution time, it should be possible to generate the 1D model through a consistent radial collapsing procedure. The 1D model obtained as such can then reproduce exactly the 3D results at least at the reference conditions on which the 1D model is based on. However, this is possible only when the steady state and transient solution methods of the 1D kinetics module are consistent with the base 3D kinetics module.

In this paper a new correction factor in a 1D model is proposed that makes the 1D model consistent with the nonlinear analytic nodal 3D model[1]. In the following sections the correction factor called current conservation factor (CCF) is derived for the 1D model consistent with 3D model. CCF is generated at the same time when the planar 1D cross sections are collapsed through the base 3D code and tested for three kinds of steady state cases and a fast transient problem.

II. Derivation of One-Dimensional Kinetics Solution Method

The 1D kinetics equation can be derived by integrating the 3D time-dependent neutron diffusion equation over the radial domain. The solution of the 1D kinetics equation is relatively simple because it involves only a block tridiagonal linear system which can be solved directly by the Gaussian elimination scheme. In order to retain good spatial solution accuracy, the nonlinear analytic nodal method (ANM) implemented in the 3D code PARCS[1] is used in the 1D solver. The 1D kinetics equation is derived rigorously and planar averaged group constants are defined. During the derivation, CCF is introduced which guarantees the same axial neutron currents to be obtained from the 1D equation as the 3D reference values. With the planar averaged group constants and CCF's, it becomes possible to reproduce the 3D reference solution from the 1D model. In order to obtain planar cross sections as functions of state parameters such as fuel temperature, moderator density and boron concentration, a generalized tabular cross section representation schemes is considered. The detailed solution methods for the eigenvalue and the transient fixed source problems as well as the temporal discretization methods are omitted here since they are already documented well in the reference [1].

II.A Derivation of One-Dimensional Kinetics Equation

The 3D time-dependent two-group neutron diffusion equation in Cartesian coordinate reads:

$$\frac{1}{v_g} \frac{\partial \mathbf{f}_g}{\partial t} = \mathbf{Q}_g - \left(\frac{\partial J_{gx}}{\partial x} + \frac{\partial J_{gy}}{\partial y} + \frac{\partial J_{gz}}{\partial z} + \Sigma_{rg} \mathbf{f}_g \right) \quad (1)$$

where

$$J_{gu} = -D_g \frac{\partial \mathbf{f}_g}{\partial u} \quad (2)$$

and

$$Q_g = \begin{cases} (1 - \mathbf{b})(\mathbf{n}\bar{\Sigma}_{f1}\mathbf{f}_1 + \mathbf{n}\bar{\Sigma}_{f2}\mathbf{f}_2) + \sum_{k=1}^K \mathbf{l}_k C_k, & g = 1 \\ \Sigma_{t2}\mathbf{f}_1, & g = 2 \end{cases} \quad (3)$$

Before integrating Eq. (1) over the radial domain, we factorize the flux into two independent functions, which are defined as the 1D flux (ϕ) and radial shape function (Φ), respectively, as the following:

$$\mathbf{f}_g(x, y, z, t) = \mathbf{j}_g(z, t)\Phi_g(x, y, z, t). \quad (4)$$

Integration of the left hand side (LHS) of Eq. (1) can then be performed using the factorized flux:

$$\begin{aligned} \int_A \frac{1}{v_g} \frac{\partial \mathbf{f}_g}{\partial t} dA &= \int_A \frac{1}{v_g} \left(\Phi_g \frac{\partial \mathbf{j}_g}{\partial t} + \mathbf{j}_g \frac{\partial \Phi_g}{\partial t} \right) dA \\ &= \frac{\partial \mathbf{j}_g}{\partial t} \int_A \frac{\Phi_g}{v_g} dA + \mathbf{j}_g \frac{\partial}{\partial t} \int_A \frac{\Phi_g}{v_g} dA \end{aligned} \quad (5)$$

In the above derivation, it was assumed that the neutron velocities are time-independent. Since Eq. (4) is an arbitrary factorization, it is possible to impose a constraint on the radial shape function to make the factorization unique. The constraint is chosen such that Eq. (5) can be simplified. Namely,

$$\int_A \frac{\Phi_g}{v_g} dA = \frac{A}{\bar{v}_g(z)} \equiv \int_A \frac{1}{v_g(x, y)} dA \quad (6)$$

where A is the area of the radial domain. The second term on the right hand side(RHS) in Eq. (5) vanishes because the integral term is constant over time and the LHS term reduces to:

$$\int_A \frac{1}{v_g} \frac{\partial \mathbf{f}_g}{\partial t} dA = \frac{A}{\bar{v}_g} \frac{\partial \mathbf{j}_g}{\partial t} \quad (7)$$

The integration of the removal term on the RHS of Eq. (1) becomes:

$$\int_A \Sigma_{rg} \mathbf{f}_g dA = \mathbf{j}_g \int_A \Sigma_{rg} \Phi dA = A \bar{\Sigma}_{rg} \mathbf{j}_g \quad (8)$$

where the planar averaged removal cross section is defined as:

$$\bar{\Sigma}_{rg} \equiv \frac{1}{A} \int_A \Sigma_{rg} \Phi_g dA \quad (9)$$

The other types of planar averaged cross sections appearing in the source terms (Q_g)

can be defined similarly.

The integration of the radial leakage term is simplified by the Gauss theorem as:

$$\begin{aligned} \int_A \left(\frac{\partial J_{gx}}{\partial x} + \frac{\partial J_{gy}}{\partial y} \right) dA &= \oint_B J_{gx} dy + \oint_B J_{gy} dx \\ &= \mathbf{j}_g \left(\oint_B -D_g \frac{\partial \Phi_g}{\partial x} dy + \oint_B -D_g \frac{\partial \Phi_g}{\partial y} dx \right) = A \Sigma_{Lg} \mathbf{j}_g \end{aligned} \quad (10)$$

where Σ_{Lg} is the leakage cross section defined as:

$$\Sigma_{Lg} = \frac{1}{A \mathbf{j}_g} \left(\oint_B J_{gx} dy + \oint_B J_{gy} dx \right) \quad (11)$$

The integration of the axial leakage term proceeds first by decomposing the axial current term as:

$$J_{gz} = -D_g \frac{\partial \mathbf{f}_g}{\partial z} = -D_g \left(\mathbf{j}_g \frac{\partial \Phi_g}{\partial z} + \Phi_g \frac{\partial \mathbf{j}_g}{\partial z} \right) . \quad (12)$$

The integration now yields:

$$\begin{aligned} \int_A \frac{\partial J_{gz}}{\partial z} dA &= \frac{\partial}{\partial z} \int_A -D_g \left(\Phi_g \frac{\partial \mathbf{j}_g}{\partial z} + \mathbf{j}_g \frac{\partial \Phi_g}{\partial z} \right) dA \\ &= -\frac{\partial}{\partial z} \int_A D_g \Phi_g dA \frac{\partial \mathbf{j}_g}{\partial z} - \frac{\partial}{\partial z} \left(\mathbf{j}_g \int_A D_g \frac{\partial \Phi_g}{\partial z} dA \right) . \end{aligned} \quad (13)$$

The first term in the RHS of Eq. (13) can be simplified by introducing the planar averaged diffusion coefficient defined as:

$$\bar{D}_g \equiv \frac{1}{A} \int_A D_g \Phi_g dA . \quad (14)$$

The second term is, however, not easy to simplify. This term would be zero if $\frac{\partial \Phi_g}{\partial z} = 0$, namely, the radial flux shape is uniform over the axial direction, which is not the normal case. By keeping this term explicitly by the following definition of shape dependent current:

$$\tilde{J}_g \equiv -\frac{\mathbf{j}_g}{A} \int_A D_g \frac{\partial \Phi_g}{\partial z} dA , \quad (15)$$

Eq. (13) reduces to:

$$\int_A \frac{\partial J_{gz}}{\partial z} dA = A \frac{\partial}{\partial z} (\bar{J}_g + \tilde{J}_g) \quad (16)$$

where

$$\bar{J}_g \equiv -\bar{D}_g \frac{\partial \mathbf{j}_g}{\partial z} . \quad (17)$$

By using Eq. (7), Eq. (8), Eq. (10), and Eq. (16), the 1D kinetics equation is now obtained as follows (after removing A from both sides):

$$\frac{1}{\bar{v}_g} \frac{\partial \mathbf{j}_g}{\partial t} = \bar{Q}_g - \left(\hat{\Sigma}_{rg} \mathbf{j}_g + \frac{\partial}{\partial z} \hat{J}_g \right) \quad (18)$$

where the effective removal cross section, $\hat{\Sigma}_{rg}$, is defined as follows by adding the radial leakage cross section:

$$\hat{\Sigma}_{rg} \equiv \bar{\Sigma}_{rg} + \Sigma_{Lg} \quad (19)$$

and the total axial current, \hat{J}_g , combines both components of the current, i.e. :

$$\hat{J}_g \equiv \bar{J}_g + \tilde{J}_g . \quad (20)$$

When a flux distribution is available from a reference 3D calculation, the planar averaged group constants can be obtained by evaluating Eq. (6), Eq. (9), Eq. (11) and Eq. (14) for each plane. If the current due to the difference in the radial shape (\tilde{J}_g), which are small compared to the current due to the difference in the 1D flux (\bar{J}_g), is neglected, then Eq. (18) can be solved for the 1D flux, \mathbf{j}_g . In such case, however, it is not possible to reproduce exactly the 3D base values of the eigenvalue and the axial flux distribution in the 1D calculation.

A problem arises when \tilde{J}_g is explicitly considered. Since this term does not contain the derivative of the 1D flux as identified in Eq. (15), inclusion of this term makes Eq. (18) no longer a diffusion equation. Moreover, since this term involves $\frac{\partial \Phi_g}{\partial z}$ which can not be evaluated in normal 3D nodal calculations, defining a collapsed group constant for the integral in Eq. (15) is not possible. In order to overcome this problem in the framework of the nonlinear nodal method, the concept of flux discontinuity is introduced here such that the total axial current (\hat{J}_g) determined in a 3D reference calculation is conserved in the 1D nodal calculation. With the discontinuity factor whose definition is detailed in the next section, it now becomes possible to reproduce exactly the 3D results in the 1D calculation at least at the reference condition and the 1D model can then be applied to other perturbed states.

II.B Two-Node Problem to Determine Current Conservation Factor

Suppose two neighboring planes for which the planar averaged group constant, fluxes, and interface currents were obtained from a 3D nodal calculation. For these two

planes, it is possible to formulate a two-node problem to determine the nodal coupling relation which is used to represent the interface current in terms of two node (or planar) averaged fluxes as:

$$J_g = -\tilde{D}_g(\mathbf{j}_g^t - \mathbf{j}_g^b) - \hat{D}_g(\mathbf{j}_g^t + \mathbf{j}_g^b) \quad (21)$$

$$\tilde{D}_g = \frac{2\bar{D}_g^t \bar{D}_g^b}{\bar{D}_g^t \Delta h_z^b + \bar{D}_g^b \Delta h_z^t} \quad (22)$$

where the superscripts t and b stand for top and bottom node of the two nodes, respectively and \tilde{D}_g means the base nodal coupling coefficients based on finite difference approximation. In normal two-node problem, the interface current as well as the correctional nodal coupling coefficient (CNCC), \hat{D}_g , is the free parameter to be determined from the two-node nodal calculation. In order to solve the normal two-node problem, four constraints are imposed per group. They are two node average fluxes and flux and current continuity at the interface. In a two-node problem, however, the interface current is not a free parameter, rather it is considered as an additional constraint.

The two-group ANM solution for a node is given by the following (refer to Section 4.2 of the reference [1] for the details of the derivation of the ANM solution):

$$\begin{aligned} \begin{bmatrix} \mathbf{j}_1(u) \\ \mathbf{j}_2(u) \end{bmatrix} &= \begin{bmatrix} \mathbf{j}_1^H(u) + \mathbf{j}_1^P(u) \\ \mathbf{j}_2^H(u) + \mathbf{j}_2^P(u) \end{bmatrix} \\ &= \begin{bmatrix} r & s \\ 1 & 1 \end{bmatrix} \begin{bmatrix} a_{21} sn(\mathbf{k}u) + a_{22} cn(\mathbf{k}u) \\ a_{23} sn(\mathbf{m}u) + a_{24} cn(\mathbf{m}u) \end{bmatrix} + \begin{bmatrix} c_{10} + c_{11}f_1(\mathbf{x}) + c_{12}f_2(\mathbf{x}) \\ c_{20} + c_{21}f_1(\mathbf{x}) + c_{22}f_2(\mathbf{x}) \end{bmatrix}, u = x, y, z \end{aligned} \quad (23)$$

In the above equation, the c coefficients are determined by the transverse leakage and/or the transient fixed source, which are zero in the 1D steady-state case. The basis functions above are represented concisely in terms of two generic functions defined below and here the first argument, m , signifies the mode of buckling.:

$$sn(m, \mathbf{I}k_\infty, u) \text{ or } cn(m, \mathbf{I}k_\infty, u) \equiv \begin{cases} \sin(u) \text{ or } \cos(u) & , \text{if } m = 0 \text{ and } \mathbf{I}k_\infty > 1 \\ u \text{ or } 1 & , \text{if } m = 0 \text{ and } \mathbf{I}k_\infty = 1 \\ \sinh(u) \text{ or } \cosh(u) & , \text{if } m = 1 \text{ or } \mathbf{I}k_\infty < 1 \end{cases} \quad (24)$$

In a two-node problem, there are then eight coefficients (2×4 a 's) to be determined. In order to determine them uniquely, the eight constraint conditions must be specified and two of them are the flux continuity condition for two groups which reads (the others are four node-average flux constraints - 2 nodes \times 2 groups - and two current continuity conditions - 2 groups):

$$\mathbf{z}_g^b \mathbf{j}_g^b \left(\frac{h_z^b}{2} \right) = \mathbf{z}_g^t \mathbf{j}_g^t \left(-\frac{h_z^t}{2} \right) \quad (25)$$

where \mathbf{z}_g is the discontinuity factor that is assumed to be known in normal two-node calculations.

If the two interface currents (one for each group) are added as the additional condition in the two-node problem, then two additional unknowns should be introduced. For this purpose, it is possible to represent the discontinuity factors as follows:

$$\mathbf{z}_g^b = 1 - \mathbf{e}_g \quad ; \quad \mathbf{z}_g^t = 1 - \mathbf{e}_g \quad (26)$$

and to take \mathbf{e}_g , which is called as CCF, as the additional unknown for each group. The ten unknowns can then be simultaneously determined by imposing the ten constraints.

The homogeneous solution for the two node problem (note that in the 1D steady-state problem, there is no particular solution because the transverse leakage is zero) can be represented as follows in terms of the several basis functions which differs depending on the magnitude of k_∞ :

$$\mathbf{j}_g^H(z) \in \begin{cases} \{\sin(\mathbf{k}z), \cos(\mathbf{k}z), \sinh(\mathbf{m}), \cosh(\mathbf{m})\} & , \quad k_\infty > k_{eff} \\ \{z, 1, \sinh(\mathbf{m}), \cosh(\mathbf{m})\} & , \quad k_\infty = k_{eff} \\ \{\sinh(\mathbf{k}z), \cosh(\mathbf{k}z), \sinh(\mathbf{m}), \cosh(\mathbf{m})\} & , \quad k_\infty < k_{eff} \end{cases} \quad (27)$$

In a two-node problem, the homogeneous solution can be compactly represented as:

$$\begin{bmatrix} \mathbf{j}_1^q(z) \\ \mathbf{j}_2^q(z) \end{bmatrix} = \begin{bmatrix} r^q & s^q \\ 1 & 1 \end{bmatrix} \begin{bmatrix} a_1^q \text{sn}(\mathbf{k}^q z) + a_2^q \text{cn}(\mathbf{k}^q z) \\ a_3^q \text{sn}(\mathbf{m}^q z) + a_4^q \text{cn}(\mathbf{m}^q z) \end{bmatrix} \quad \text{for } q = b \text{ or } t \quad (28)$$

The total 10 unknowns composed of 8 coefficients of the two nodes and 2 CCF's can be solved with the following constraints:

1) node average fluxes conservation:

$$\bar{\mathbf{J}}_g^q = \frac{1}{h^q} \int_{-h^q/2}^{h^q/2} \mathbf{j}_g^q(z) dz \quad \text{for } q = b, t; \quad g = 1, 2 \quad . \quad (29)$$

2) surface average current conservation at the interface:

$$\begin{aligned} \bar{J}_g^{3D}(z) &= -\bar{D}_g^b(z) \frac{d}{dz} \mathbf{j}_g^b(z) \Big|_{z=h^b/2} \\ &= -\bar{D}_g^t(z) \frac{d}{dz} \mathbf{j}_g^t(z) \Big|_{z=-h^t/2} \end{aligned} \quad (30)$$

3) flux continuity using CCF factors at the interface:

$$(1 - \mathbf{e}_g) \mathbf{j}_g^b \left(\frac{h_z^b}{2} \right) = (1 + \mathbf{e}_g) \mathbf{j}_g^t \left(-\frac{h_z^t}{2} \right) \quad (31)$$

Note that there are additional constraints in Eq. (30) which requires the current determined in the two node problem be the same as the average current obtained from the reference 3D calculation. The above constraints constitute 10 equations that can be solved for 10 unknowns.

The final solution form should be different depending on the basis function which is determined by the node properties. Here, the solution is provided only for the case that the base functions are $\sin(z)$ and $\cos(z)$ corresponding to $m=0$, $Ik_\infty > 1$. The eight coefficients determined from the simultaneous solution of the 10 equations are as follows:

$$a_1^b = \frac{\sec(h^b \mathbf{k}^b / 2)(2\bar{D}_1^b \bar{J}_2^{3D} s^b + \bar{D}_2^b (-2\bar{J}_1^{3D} + \bar{D}_1^b h^b (\mathbf{k}^b)^2 (\bar{\mathbf{J}}_1^b - s^b \bar{\mathbf{J}}_2^b))}{2\bar{D}_1^b \bar{D}_2^b (r^b - s^b) \mathbf{k}^b}, \quad (32)$$

$$a_1^t = \frac{\sec(h^t \mathbf{k}^t / 2)(2\bar{D}_1^t \bar{J}_2^{3D} s^t + \bar{D}_2^t (-2\bar{J}_1^{3D} + \bar{D}_1^t h^t (\mathbf{k}^t)^2 (-\bar{\mathbf{J}}_1^t + s^t \bar{\mathbf{J}}_2^t))}{2\bar{D}_1^t \bar{D}_2^t (r^t - s^t) \mathbf{k}^t}, \quad (33)$$

$$a_3^b = \frac{\sec h(h^b \mathbf{m}^b / 2)(-2\bar{D}_1^b \bar{J}_2^{3D} r^b + \bar{D}_2^b (2\bar{J}_1^{3D} + \bar{D}_1^b h^b (\mathbf{m}^b)^2 (\bar{\mathbf{J}}_1^b - r^b \bar{\mathbf{J}}_2^b))}{2\bar{D}_1^b \bar{D}_2^b (r^b - s^b) \mathbf{m}^b}, \quad (34)$$

$$a_3^t = \frac{\sec h(h^t \mathbf{m}^t / 2)(-2\bar{D}_1^t \bar{J}_2^{3D} r^t + \bar{D}_2^t (2\bar{J}_1^{3D} + \bar{D}_1^t h^t (\mathbf{m}^t)^2 (-\bar{\mathbf{J}}_1^t + r^t \bar{\mathbf{J}}_2^t))}{2\bar{D}_1^t \bar{D}_2^t (r^t - s^t) \mathbf{m}^t}, \quad (35)$$

$$a_2^b = \frac{\csc(h^b \mathbf{k}^b / 2) h^b \mathbf{k}^b (\bar{\mathbf{J}}_1^b - s^b \bar{\mathbf{J}}_2^b)}{2(r^b - s^b)}, \quad (36)$$

$$a_2^t = \frac{\csc(h^t \mathbf{k}^t / 2) h^t \mathbf{k}^t (\bar{\mathbf{J}}_1^t - s^t \bar{\mathbf{J}}_2^t)}{2(r^t - s^t)}, \quad (37)$$

$$a_4^b = \frac{\csc h(h^b \mathbf{m}^b / 2) h^b \mathbf{m}^b (-\bar{\mathbf{J}}_1^b + r^b \bar{\mathbf{J}}_2^b)}{2(r^b - s^b)}, \quad (38)$$

$$a_4^t = \frac{\csc h(h^t \mathbf{m}^t / 2) h^t \mathbf{m}^t (-\bar{\mathbf{J}}_1^t + r^t \bar{\mathbf{J}}_2^t)}{2(r^t - s^t)} \quad (39)$$

The final expression for CCF is then obtained follows:

$$\mathbf{e}_g = \frac{\mathbf{j}_g^b (h^b / 2) - \mathbf{j}_g^t (-h^t / 2)}{\mathbf{j}_g^b (h^b / 2) + \mathbf{j}_g^t (-h^t / 2)}, \quad g = 1, 2 \quad (40)$$

III Test Problems

CCF values derived in the previous section are generated when the 1D cross section set is prepared with planar collapsed cross section. And they are used when solving the intra nodal flux distribution in a two node problem kernel of 1D model.

In order to test the effect of CCF, three kinds of steady state calculations and a fast transient problem are performed. The test core is based on NEACRP benchmark problem. The axial flux(power) distribution is mainly distorted by the control rod insertion, so the test cases are selected as case 1; all rod out case, case 2; rods inserted half to the active core height and case 3; several rods are inserted sequentially. And the NEACRP benchmark A1 problem[4] that simulates the fast core transients due to a

central rod ejection.

IV Results and Conclusion

Table 1 shows the CCF values obtained from the three test cases. Table 2 shows the results of K-eff values compared with the 3D reference value when the CCF is used and not used. The errors of K-eff values are reduced about one tenth when using CCF. Tables 3 and 4 show the comparison results of peak power and peripheral power. The axial power distribution from 1D calculation agrees well to that of 3D reference value as shown in Figure 1. The errors of power are decreased to the range of one fifth or tenth in the case using CCF. However as shown in Figure 2, CCF does not effect much on the overall core behavior result in a case of fast transient such as a rod ejection. Because the major factor determining the core behavior in a fast rod ejection problem initiated from a heavily rodded condition is the total rod worth involving a transient. With the planar averaged group constants and CCF's, it becomes possible to reproduce the 3D reference solution from the 1D model. Thus the 1D model with CCF can provide the preciser results at the steady state, and it is expected that the slow transient such as the day range xenon dynamics can be simulated more accurately with 1D model.

V References

1. H. G. Joo et al, "PARCS A Multi-dimensional Two-Group Reactor Kinetics Code Based on the Nonlinear Analytic Nodal Method," *PU/NE-97-4*, Purdue University, (1997).
2. Kibog Lee, H. G. Joo, and Sung Qunn Zee, "Software Design and Implementation Document for the One-Dimensional Kinetics Module of TRAC-M/PARCS," (*to be published*), KAERI and PURDUE University, (1999).
3. H. G. Joo, Kibog Lee, and Sung Qunn Zee, "Software Requirements Specification for the One-Dimensional Kinetics Module for TRAC-M/PARCS," KAERI and PURDUE University, (1999).
4. H. Finnemann et al, "Results of LWR Core Transient Benchmarks," *Proc. Intl. Conf. Math. Meth. Supercomput. Nucl. Appl.*, Karlsruhe, pp. 243-258, April 1993.

Table 1. Sample of CCF values

Node No.	Case-1		Case-2		Case-3	
	CCF-1	CCF-2	CCF-1	CCF-2	CCF-1	CCF-2
2	3.922047E-02	3.792532E-02	3.932028E-02	3.799754E-02	4.095733E-02	3.965351E-02
3	1.402784E-03	1.540256E-03	1.401115E-03	1.526394E-03	1.460416E-03	1.692759E-03
4	6.207732E-04	1.281259E-03	6.067341E-04	1.238928E-03	6.193009E-04	1.354002E-03
5	7.097761E-04	1.247093E-03	6.572262E-04	1.142919E-03	6.553792E-04	1.406484E-03
6	4.847944E-04	7.626906E-04	3.002599E-04	4.897273E-04	5.145261E-05	6.294915E-04
7	2.859150E-04	4.469273E-04	5.295197E-05	9.835972E-05	-4.922900E-04	-3.372619E-05
8	1.689825E-04	2.624045E-04	-1.926969E-04	-2.936846E-04	-5.825792E-04	-8.159370E-04
9	7.776116E-05	1.208078E-04	1.470752E-04	3.410101E-04	-4.909438E-04	-1.378600E-03
10	-2.420514E-06	-3.479503E-06	2.128189E-04	1.172492E-03	-1.158163E-03	-2.673722E-03
11	-8.231506E-05	-1.273399E-04	-3.193745E-03	-7.698134E-03	-2.277768E-03	-3.021050E-03
12	-1.749327E-04	-2.703663E-04	-9.997496E-03	-1.439397E-02	-2.921803E-03	-3.646835E-03
13	-2.939006E-04	-4.556907E-04	-5.189781E-03	-8.247424E-03	-2.120458E-03	-2.667255E-03
14	-4.968247E-04	-7.686452E-04	-7.415104E-03	-1.050758E-02	-1.097869E-03	-1.046316E-03
15	-7.109716E-04	-1.232297E-03	-2.313249E-03	-4.181173E-03	-2.601829E-03	-5.937549E-03
16	-6.252996E-04	-1.352798E-03	-9.782316E-04	-2.300859E-03	-1.345732E-03	-3.896898E-03
17	-1.613005E-03	-1.334228E-03	-2.025886E-03	-3.963753E-03	-2.356987E-03	-5.068253E-03
18	-3.987261E-02	-3.330637E-02	-4.307671E-02	-3.804341E-02	-4.868531E-02	-4.426072E-02

Table 2. Comparison of Core Eigenvalue(K-eff) at Steady State

Method		Case-1	Case-2	Case-3
3D reference	K-eff	1.087519	1.078697	1.075649
1D without CCF	K-eff	1.087554	1.078791	1.075771
	Error(pcm) *	-3.5	-9.4	-12.2
1D with CCF	K-eff	1.087522	1.078706	1.075660
	Error(pcm) *	-0.3	-0.9	-1.1

* : Error = (3D – 1D)*100000

Table 3. Comparison of Maximum Axial Power at Steady State

Method		Case-1	Case-2	Case-3
3D reference	Peak	1.5097(9)	2.5804(7)	2.2552(7)
1D without CCF	Peak	1.5058(9)	2.5727(7)	2.2506(7)
	Error(%) *	-0.256	-0.300	-0.202
1D with CCF	Peak	1.5092(9)	2.5793(7)	2.2543(7)
	Error(%) **	-0.033	-0.046	-0.039

** : Error = (3D – 1D)/3D*100

(#) means the peak node number

Table 4. Comparison of Peripheral Node Power at Steady State

Method		Case-1	Case-2	Case-3
3D reference	Node Power	0.1637(2)	0.4954(2)	0.4776(2)
1D without CCF	Node Power	0.1729(2)	0.5235(2)	0.5072(2)
	Error(%) **	5.591	5.657	6.202
1D with CCF	Node Power	0.1654(2)	0.5005(2)	0.4828(2)
	Error(%) **	1.027	1.024	1.082

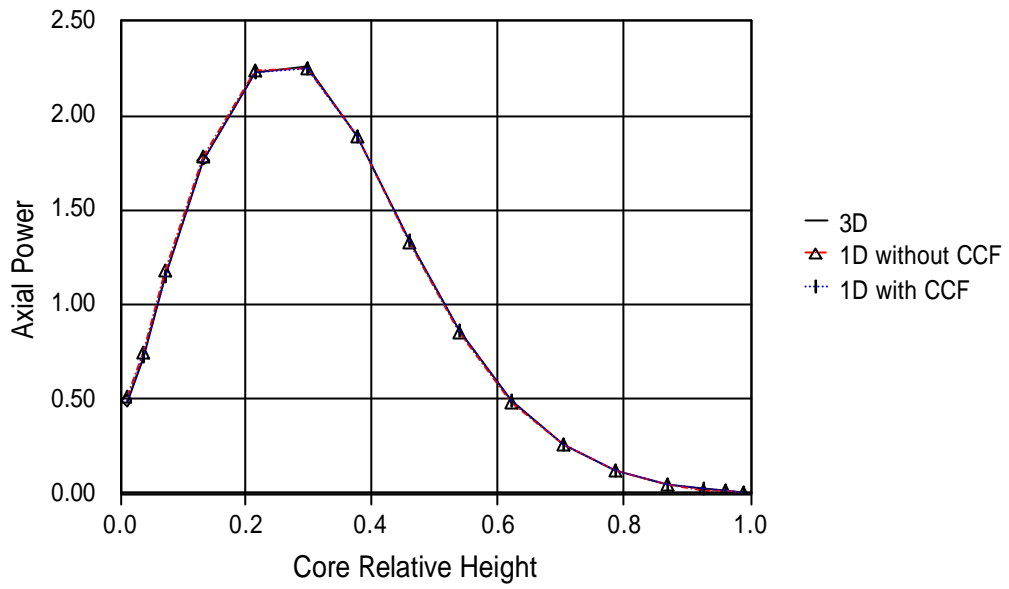


Figure 1. Comparison of Axial Power Distribution(Case-3)

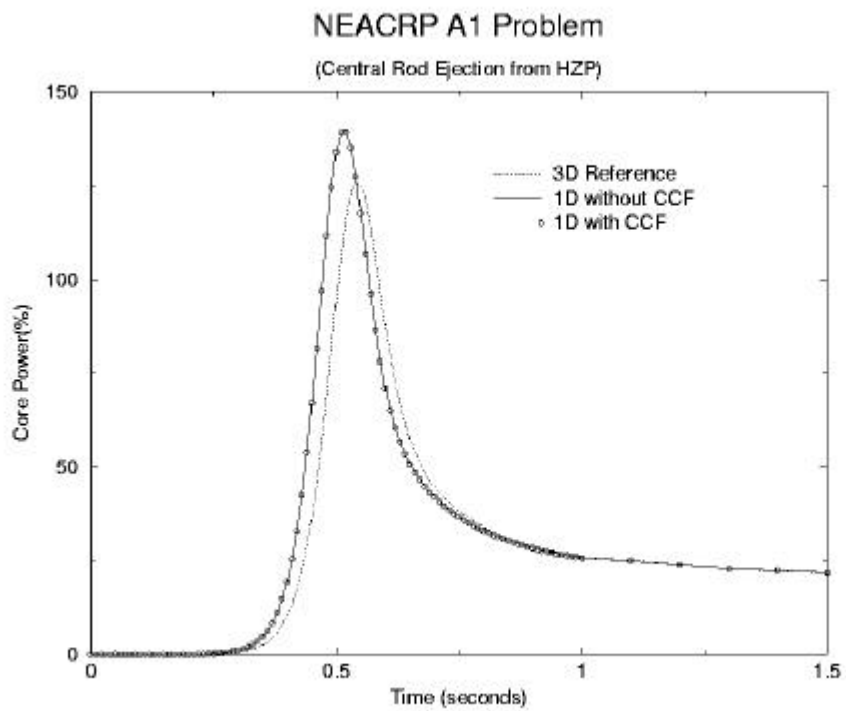


Figure 2. Comparison of Fast Transient Result for NEACRP A1 Problem